

A new method based on the subpixel Gaussian model for accurate estimation of asteroid coordinates

Savanevych, V. E.^{1*}, Briukhovetskyi, O. B.², Sokovikova, N. S.¹, Bezkrovny, M. M.³, Vavilova, I. B.⁴, Ivashchenko, Yu. M.^{4,5}, Elenin, L. V.⁶, Khlamov, S. V.¹, Movsesian, Ia. S.¹, Dashkova, A. M.³, Pogorelov A. V.¹

¹Kharkiv National University of Radio Electronics, 14 Lenin ave., Kharkiv 61166, Ukraine

²Kharkiv Representation of the General Customer's Office of the State Space Agency of Ukraine, 1 Akademika Proskury St., Kharkiv 61070, Ukraine

³Zaporizhya Institute of Economics and Information Technologies, 16-B Kiyashka St., Zaporizhya 69015, Ukraine

⁴Main Astronomical Observatory of the NAS of Ukraine, 27 Akademika Zabolotnogo St., Kyiv 03680, Ukraine

⁵Andrushivka Astronomical Observatory, Galchyn, Zhomyr Region 13400, Ukraine

⁶Keldysh Institute of Applied Mathematics of the RAS, 4 Miusskaya sq., Moscow 125047, Russian Federation

11 September 2018

ABSTRACT

We describe a new iteration method to estimate asteroid coordinates, which is based on the subpixel Gaussian model of a discrete object image. The method operates by continuous parameters (asteroid coordinates) in a discrete observational space (the set of pixels potential) of the CCD frame. In this model, a kind of the coordinate distribution of the photons hitting a pixel of the CCD frame is known a priori, while the associated parameters are determined from a real digital object image. The developed method, being more flexible in adapting to any form of the object image, has a high measurement accuracy along with a low calculating complexity due to a maximum likelihood procedure, which is implemented to obtain the best fit instead of a least-squares method and Levenberg-Marquardt algorithm for the minimisation of the quadratic form.

Since 2010, the method was tested as the basis of our CoLiTec (Collection Light Technology) software, which has been installed at several observatories of the world with the aim of automatic discoveries of asteroids and comets on a set of CCD frames. As the result, four comets (C/2010 X1 (Elenin), P/2011 NO1(Elenin), C/2012 S1 (ISON), and P/2013 V3 (Nevski)) as well as more than 1500 small Solar System bodies (including five NEOs, 21 Trojan asteroids of Jupiter, and one Centaur object) were discovered. We discuss these results that allowed us to compare the accuracy parameters of a new method and confirm its efficiency.

In 2014, the CoLiTec software was recommended to all members of the Gaia-FUN-SSO network for analysing observations as a tool to detect faint moving objects in frames.

Key words: methods: data analysis; minor planets, asteroids, comets; techniques: image processing.

1 INTRODUCTION

There are many methods for determining an asteroid position during observations with a CCD camera. For example, the Full Width at Half Magnitude (FWHM) approach (Gary & Healy 2006), which is based on the analytical description of the object images on the CCD frame, as well as other methods, in which the position of an object's maximum brightness on a CCD image is taken as its coordinates (Miura et al. (2005)).

Most of these methods have a common feature. They use

PSF-fitting (Point-Spread Function) to approximate the object image and get the information about regularities in the distribution of the registered photons on CCD frame(see, for detail, Yanagisawa et al. (2005), Gural et al. (2005), Veres and Jedicke (2012), Dell'Oro et al. (2012), Lafreniere et al. (2007), Zacharias (2010)), Among the models of photons distribution, which are used more often, we note the two-dimensional Gaussian model (Veres and Jedicke (2012), Zacharias (2010), Jogesh Babu et al. (2008)), Moffat model (Bauer (2009), Izmailov et al. (2010)) or Lorentz model (Zacharias (2010), Izmailov et al. (2010)). These models are usually described by the continuous functions, while the CCD images are discrete ones. Such an approach was criticised rea-

* vadym@savanevych.com

sonably by Bauer (2009). The principal disadvantage is that these models work well only with a large amount of the data. It leads to the fact that, firstly, the computation process becomes much more complicated, and, secondly, the problem related with the adequacy of the used estimations of PSF parameters cannot be solved. As a result, the error of the coordinate determination of the observed celestial objects has to be increasing.

In addition to the aforementioned disadvantage, the existing methods do not pay sufficient attention for taking the noise component of the object image into account. It is assumed that its registration and compensation are performed during the preliminary stage of image processing (Gural et al. (2005)) or that the object image is exempted from noise according to the accepted signal-to-noise model (Lafreniere et al. (2007), Izmailov et al. (2010)). At the same time, the error introduced by the operation of removing the noise component from the object image is not considered in the subsequent procedure of coordinate determination.

The errors of CCD astrometry are traditionally divided into the instrument, reduction, reference catalogue and measurement errors.

The first ones traditionally include errors of instrumental parameters as shutter delay and clock correction, which result in incorrect timing. The second error category (reduction) is associated with the method related to the standard and measured coordinates and depends on the choice of the algorithm relation between these coordinates. For example, being not sufficient for the wide-angle astrographs such an error depends strongly on the choice of the type and degree of the polynomial approximation in Turner method. It is important to note that a systematic error of timing is not shared with the coordinate error along the tracking an object in the sky, so it must be caught clearly with a reliable shutter sync.

The reference catalogue errors are divided into three main classes: zonal errors (systematic errors of the reference catalogue); coordinate errors of reference stars in the catalogue epoch; proper motion errors of reference stars. Therefore, a choice of the reference catalogue is very important. For example, Hipparcos or Tycho catalogues had no errors in the epoch of 1990.0, because an intrinsic accuracy was at the level of millisecond of arc, but for the present epoch there is a necessity to take into account the proper motion errors of reference stars. The solution of this problem, i.e., creation of new huge database of proper motions of stars, is one of the task of the GAIA mission. It is worth noting that the choice of reference catalogue is not so important, when monitoring observations of sky are conducted with the aim of discovery of new Solar system small bodies, because an intrinsic accuracy of a catalogue should not be necessarily maximised as compared with those for the following tracking the discovered object.

The measurement error is related, first of all, to the determination of coordinates of the image centre or the accuracy of a digital approximation of the CCD image (fitting). The attempt to improve the fitting may not lead to expected results if the reference catalogue errors and timing are not taken attentively into account.

Each of the aforementioned factors could be the source of both systematic and random errors. Any attempt to reduce one of these errors is impossible without control of other factors. Therefore, the task of the observers is to be responsible for monitoring all the possible sources of errors. The aim of this paper is to help the observers to refine the coordinate measurements of the object image on the CCD frame and to control the errors of the measured coordinates.

With this aim, we developed a new method for accurately estimating asteroid coordinates on a set of CCD frames, which is based on the subpixel Gaussian model of the discrete image of an object. In this model, a kind of the coordinate distribution of the photons

hitting a pixel on the CCD frame is known a priori, while its parameters can be determined from the real digital image of the object. Our method has low computational complexity due to the use of equations of maximum likelihood, as well as the proposed model is more flexible, adapting to any form of the real image of the object. For example, in fact PSF is a super-pixel function because it describes the changes in the brightness of a pixels of celestial object image. We propose to use the density function of coordinates of hitting photons from celestial object instead of the PSF. This function is sub-pixel one. To get the Point-Spread Function from this function, it should be integrated over the area of determination of each image pixel of object or compact group of objects. It turns out that sub-pixel models are more flexible and may describe the real image more adequately. This effect does not occur in case of bright objects. But applying a more flexible model for the faint objects, we are able to improve the accuracy of the measurements (for example, as comparing with Astrometrica) by 30-50% (more details are given in the discussion). Our method also takes into account the principal peculiarities of the object image formation on the CCD frame along with the possible irregular distribution of the residual noise component both on the object image and in its vicinity.

Some generalisations of the proposed method are presented in our previous works (Savanevych (1999), Savanevych (2006), Savanevych et al. (2010), Savanevych et al. (2011) Vavilova et al. (2011), Savanevych et al. (2012), Vavilova et al. (2012(a)), Vavilova et al. (2012(b)), Savanevych et al. (2014)). Since 2010, due to its application with the CoLiTec (Collection Light Technology) software, which was installed at several observatories of the world, four comets (C/2010 X1 (Elenin), P/2011 NO1(Elenin), C/2012 S1 (ISON), and P/2013 V3 (Nevski)) and more than 1500 small Solar System bodies (including five NEOs, 21 Trojan asteroids of Jupiter, and one Centaur object) were discovered. These results confirm the efficiency of the proposed method. The main stages of image processing with the CoLiTec software are presented in Fig. 1.

The structure of this article is as follows: we describe a problem statement and the method in Chapters 2-3, respectively. The results based on the testing of this method with the CoLiTec software are presented in Chapter 4. We compare and discuss the accuracy and other parameters for determining the position of the faint celestial object on the CCD frame obtained by the proposed method and others in Chapter 5. Conclusive remarks are given in Chapter 6.

2 PROBLEM STATEMENT

If the exposure time is small, the shift of asteroid position in the sky can be ignored. In this case, the asteroid and field stars are imaged as blur spots rather than points on the CCD frame. It is postulated that the coordinates of the signal photons from asteroids and stars hitting the CCD frame have a circular normal distribution with mathematical expectations x_t , y_t and mean-square error (MSE) σ_{ph} .

It is supposed that a preliminary detection of asteroid has already been conducted before the determination of its coordinates. The result of this detection is a preliminary estimation of the asteroid position on the CCD frame, namely, the determination of coordinates of the pixel, which corresponds to the maximum brightness peak on the asteroid image. We name the set of pixels around this pixel as the area of intraframe processing (AIFP). Thus, the AIFP size (N_{IPS} , in pixels) is much larger than the image of the asteroid.

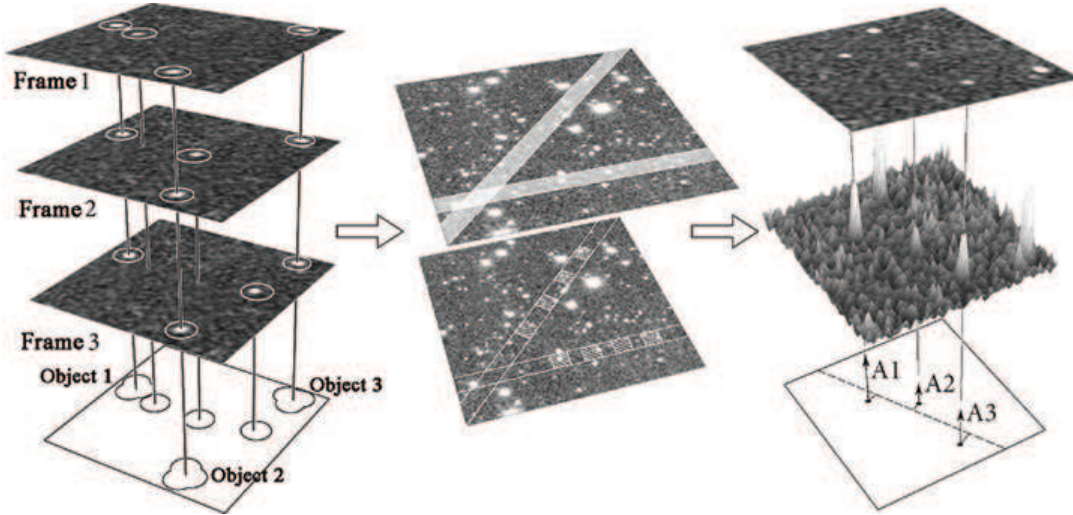


Figure 1. Main steps of object image processing in the CoLiTec software: a) exclusion of stationary objects; b) detection of moving objects; c) analysis of moving objects, where A₁, A₂, and A₃ outline coordinate deviations of moving objects from their trajectory.

The original CCD image of the celestial object contains harmful interferences such as the read noise, dark currents, irregularity in the pixel-to-pixel sensitivity, sky background radiation, etc. (Faraji and MacLean (2006), Harris (1990)). Hence, the CCD frame, can be represented as an additive mix of the images of celestial objects and a component, which is formed by this generalised interference. Within the scope of the whole CCD frame the interference component has a complex structure. However, in a small vicinity of the studied asteroid image, such interference component can be described with a good accuracy as a plane with an arbitrary slope. Such a representation describes well the interference component especially if there is a bright object near the vicinity of the studied AIFP.

The output signals of the CCD matrix pixels N_{IPS} are easily reduced to the relative frequencies ν_{ikt}^* of the photons hitting the ik^{th} pixel on the t^{th} frame:

$$\nu_{ikt}^* = \frac{A_{ikt}}{\sum_{i,k} A_{ikt}}, \quad (1)$$

where A_{ikt} is the brightness of the ik pixel of the CCD matrix.

Then, the result of the observation is the set $\tilde{U} = \nu_{11t}^*, \dots, \nu_{ikt}^*, \dots, \nu_{N_{IPS}t}^*$ of the relative frequencies, which are independent of each other. The theoretical analogues of the measured relative frequencies are the probabilities $\nu_{ikt}(\Theta)$ that during the exposure time the photons hit the ik^{th} -pixel of the CCD matrix with the borders x_{begi}, x_{endi} in the coordinate x and y_{begk}, y_{endk} in the coordinate y on the t^{th} frame. It is supposed that the angular sizes of the pixel, Δx and Δy , are the same in both coordinates x and y .

Thus, the problem statement is as follows: it is needed to develop a method of maximum likelihood estimation of asteroid coordinates on the t^{th} CCD frame using the set of relative frequencies ν_{ikt}^* . It is believed that the likelihood function is differentiable in the vicinity of its global maximum, and its initial approximation is also in the same vicinity. The set of the estimated parameters Θ includes the asteroid coordinates x_t and y_t on the t^{th} frame and the mean square error of the coordinates of photons hitting the CCD matrix, σ_{ph} .

To introduce a new method, we use two functions. The density distribution of a normally distributed random variable z with mathematical expectation m_z and dispersion σ^2 is determined by the expression:

$$N_z(m_z, \sigma^2) = \frac{1}{\sqrt{2\pi}\sigma} \exp\left(-\frac{1}{2\sigma^2}(z - m_z)^2\right). \quad (2)$$

The probability F_z that a random variable z is within the closed interval $[z_{beg}, z_{end}]$ is:

$$F_{zi}(m_z, \sigma^2) = \int_{z_{end}}^{z_{beg}} N_z(m_z; \sigma^2) dz. \quad (3)$$

3 TASK SOLUTION

For achieving the maximum accuracy of the estimations of the object position on the frame, the discretisation factor needs to be taken into account, because we should estimate the continuous parameters (coordinates of objects) at the discrete set of the measured values (the brightness of the CCD matrix pixels). The general view of the maximum likelihood estimation of the object position can be expressed by:

$$\sum_{i,k} \frac{\nu_{ikt}^*}{\nu_{ikt}(\Theta)} \frac{\partial \nu_{ikt}(\Theta)}{\partial \Theta_m} = 0, \quad (4)$$

where Θ is the set of the estimated parameters x_t, y_t , and σ_{ph} .

The relation between the probability $\nu_{ikt}(\Theta)$ that photons hit the ik^{th} pixel (Eq. 4) and the function of coordinates distribution $f(x, y)$ of the incidence of photons from the object on the CCD matrix has the form:

$$\nu_{ikt}(\Theta) = \int_{x_{begi}}^{x_{endi}} \int_{y_{begk}}^{y_{endk}} f(x, y) dx dy. \quad (5)$$

After the compensation of the noise component on the CCD

image, the function $f(x, y)$ could be expressed as the weighted mix of normal and uniform probability distributions:

$$f(x, y, \Theta) = p_0 + \frac{p_1}{2\pi\sigma_{ph}^2} \exp\left\{-\frac{1}{2\sigma_{ph}^2}[(x - x_t)^2 + (y - y_t)^2]\right\}, \quad (6)$$

where $p_1 = 1 - p_0$ is the relative weight of the signal photons of the object; p_0 ($0 \leq p_0 < 1$) is the relative weight of the residual noise photons of the CCD matrix after the compensation of the flat generalised interference; x_t and y_t are the object coordinates on the t^{th} frame at the time t^t corresponding to the mathematical expectations of the coordinates of incidence of the signal photons.

The probability (Eq. 5) that photons hit the CCD matrix pixels can be written as follows:

$$\nu_{ikt}(\Theta) = I_{iktnoise} + I_{ikts}, \quad (7)$$

where $I_{ikts} = p_i F_{xi}(x_i; \sigma_{phi}^2) F_{yk}(y_t; \sigma_{ph}^2)$ is the probability that signal photons I_{ikt} hit the ik^{th} pixel of the CCD matrix; and $I_{iktnoise} = \Delta_{CCD}^2 p_0$ is the probability that the noise residuary photons hit the ik^{th} pixel of the CCD matrix; $\Delta_{CCD} = \Delta_x = \Delta_y$.

The derivative from the probability (Eq. 7) in the x coordinate is determined by the expression:

$$\frac{d\nu_{ikt}(\Theta)}{dx_t} = \frac{p_1 F_{yk}(y_t; \sigma_{ph}^2) F_{xi}(x_t; \sigma_{ph}^2)}{\sigma_{ph}} (m_{xi}^{loc} - x_t), \quad (8)$$

where

$$m_{xi}^{loc} = m_x + \frac{\sigma^2}{F_{xi}(m_x; \sigma^2)} (N_{xendi}(m_x; \sigma^2) - N_{xbegi}(m_x; \sigma^2))$$

is the local (on the closed interval $[xbegi; xendi]$) mathematical expectation of the normally distributed random value x with a mathematic expectation m_x and dispersion σ^2 . The derivative from the probability (Eq. 7) in the y coordinate has the same expression as Eq. 8.

The system of equations of the maximum likelihood for the studied AIFP pixels in the case while the asteroid position is estimated only, will take the form:

$$\begin{cases} \hat{x}_t = \frac{\sum_{i,k}^{N_{IPSs}} \nu_{ikt}^* \lambda_{ikt} m_{xi}^{loc}}{\sum_{i,k}^{N_{IPSs}} \nu_{ikt}^* \lambda_{ikt}}; \\ \hat{y}_t = \frac{\sum_{i,k}^{N_{IPSs}} \nu_{ikt}^* \lambda_{ikt} m_{yk}^{loc}}{\sum_{i,k}^{N_{IPSs}} \nu_{ikt}^* \lambda_{ikt}}, \end{cases} \quad (9)$$

where N_{IPSs} is the quantity of pixels in the part of AIFP area (the area, where the signal from the object is expected); \hat{x}_t and \hat{y}_t are the estimations of asteroid coordinates; and λ_{ikt} is the part of photons from the celestial object in the ik^{th} pixel of the t^{th} CCD frame. The latter value is determined by:

$$\lambda_{ikt} = \frac{p_1 F_{yk}(y_t; \sigma_{ph}^2) F_{xi}(x_t; \sigma_{ph}^2)}{\nu_{ikt}(\Theta)}. \quad (10)$$

To estimate the MSE of the coordinates of the photons hitting the CCD frame from the asteroid, we use the equation of the maximal likelihood:

$$\hat{\sigma}_{ph}^2 = \frac{\sum_{i,k}^{N_{IPSs}} \nu_{ikt}^* \lambda_{ikt} ((m_{xi}^{loc} - \hat{x}_t)^2 + (m_{yk}^{loc} - \hat{y}_t)^2)}{2 \sum_{i,k}^{N_{IPSs}} \nu_{ikt}^* \lambda_{ikt}}. \quad (11)$$

We cannot exclude completely the generalised noise interference. By this reason, to take into account the relative weight of the signal photons, we use a standard estimation of the weights of the discrete mix of the probability distributions (Lo et al. (2001)):

$$\hat{p}_1 = \frac{1}{N_{IPSs}} \sum_{i,k}^{N_{IPSs}} \lambda_{ikt}; \hat{p}_0 = 1 - \hat{p}_1. \quad (12)$$

Therefore, the local mathematical expectation of coordinates of the object position is a function of the relevant coordinates, and Eq. 9 gives a system of transcendental equations that can be solved by the method of successive approximations (see, e.g., Burden and Faires (2010)).

The algorithm of the estimation of object coordinates consists of two successive operations.

The first operation is to split the statistics of the AIFP pixels into the statistics of the signal and statistics of the residual interference. It is performed for pixels from the AIFP area where the object is expected. According to the Θ values calculated from the previous iteration, the photons of pixel are divided into those belonging to the object and to the residual interference. The photons belonging to the object are analysed to determine estimation of its position. Thus, coordinates of the local maximum in the object image, around which the AIFP area is formed, are used as the initial approximation. The result of this operation is a set of split coefficients λ_{ikt} .

The second operation provides estimation of the object coordinates based on the statistics, which are obtained during the operation of splitting. It is conducted in a strongly determined way from Eq. 9 to Eq. 12. The result $\hat{\Theta}_n$ of this operation serves as an initial approximation for the operation of splitting at the next iteration step. The iteration process is continued until the difference between $\hat{\Theta}_n$ and $\hat{\Theta}_{n-1}$ becomes smaller than the predetermined value, for example, 0.1% of the angle size of a pixel.

The analysis of the iteration process shows that its convergence is provided while the following conditions are fulfilled:

$$dx = \frac{|x_0 - x_{true}|}{\sigma_x} < 6, dy = \frac{|y_0 - y_{true}|}{\sigma_y} < 6, \quad (13)$$

where dx and dy are the relative distances between the initial and actual positions of the object; x_0 and y_0 are the initial approximation of the object coordinates, x_{true} and y_{true} are the actual object coordinates; and σ_x and σ_y are the MSEs of coordinates of the signal photons hitting the CCD matrix.

The observations based on the proposed method have shown that this condition is almost always fulfilled for the real images of asteroids and stars, and, in most cases, the relative distance is not more than $1.0 \div 15$.

The opportunity to divide the AIFP area into the interference area (pixels that have registered photons only from interferences) and the object area (pixels that have registered photons from the object and interference) yields a more simple and reliable algorithm of estimation of the flat interference component (as compared with the estimation in the common system of maximum likelihood equations). Namely, there is an independent estimation by the method of least squares (MLS). Thus, the density of the coordinate distri-

bution of the photons from the residual interference will represent an equation of the plane with an arbitrary slope:

$$f_{noise}(x, y) = A_{noise}x + B_{noise}y + C_{noise}. \quad (14)$$

The probability that these photons will hit the ik^{th} pixel can be given by analogy with Eq. 5:

$$\nu_{iktnoise}^*(\Theta_{noise}) = A_{noise}^{int}x_{ik} + B_{noise}^{int}y_{ik} + C_{noise}^{int}, \quad (15)$$

where $\nu_{iktnoise}^*$ is the measured frequency of the noise photons hitting the ik^{th} pixel of the CCD matrix; $A_{noise}^{int} = \Delta_{CCD}^2 A_{noise}$, $B_{noise}^{int} = \Delta_{CCD}^2 B_{noise}$, $C_{noise}^{int} = \Delta_{CCD}^2 C_{noise}$, $\Theta_{noise}^T = (A_{noise}^{int}, B_{noise}^{int}, C_{noise}^{int})$ are the integral parameters of the flat noise component and its vectors; $x_{ik} = \frac{x_{end}+x_{beg}}{2}$, $y_{ik} = \frac{y_{endk}+y_{begk}}{2}$ are the average values of coordinates of the ik^{th} pixel.

Thus, the probabilities that noise photons will hit the pixels of the studied AIFP depend linearly on the angle coordinates of the centres x_j and y_j of these pixels and represent, by themselves, a plane with the integral parameters A_{noise}^{int} , B_{noise}^{int} and C_{noise}^{int} . It is worth noting that the pixels containing the supposed object image should be eliminated before the determination of the noise parameters.

The integral parameters of the flat interference component A_{noise}^{int} , B_{noise}^{int} and C_{noise}^{int} can be determined with a linear MLS estimation:

$$\hat{\Theta}_{noise} = (F^T F)^{-1} F^T \tilde{U}_{noise}, \quad (16)$$

where

$$F^T = \begin{vmatrix} x_1 & \dots & x_i & \dots & x_{N_{IPSnoise}} \\ y_1 & \dots & y_i & \dots & y_{N_{IPSnoise}} \\ 1 & \dots & 1 & \dots & 1 \end{vmatrix} \quad (17)$$

where x_j and y_j are the angular coordinates of the j^{th} pixel, which is used to estimate parameters of the flat interference component; $N_{IPSnoise}$ is the number of AIFP pixels, which do not contain the object image.

To obtain the integral parameters (Eq. 16 - Eq. 17), only the AIFP pixels not belonging to the areas with the object images ($N_{IPSnoise} \leq (N_{IPS} - N_{IPSS})$) should be used. To exclude the influence of the anomalous emissions of the brightness in the pixels, we apply two iterations of MLS. In the second iteration, we use only those pixels, for which the value of the obtained frequency $\nu_{iktnoise}^*$ satisfies the following condition:

$$|\nu_{iktnoise}^* - \hat{\nu}_{iktnoise}^*| \leq k_{noise} \sqrt{\frac{\sum_{i,k}^{N_{IPSnoise}} (\nu_{iktnoise}^* - \hat{\nu}_{iktnoise}^*)^2}{N_{IPSnoise}}}, \quad (18)$$

where k_{noise} is the threshold coefficient for removing the pixels, which do not satisfy this condition, for example, $k_{noise}=3$; $\sqrt{\frac{(\sum_{i,k}^{N_{IPSnoise}} (\nu_{iktnoise}^* - \hat{\nu}_{iktnoise}^*)^2)}{N_{IPSnoise}}}$ are the standard deviations of the flat interference component; and $\hat{\nu}_{iktnoise}^* = \hat{A}_{noise}^{int}x_{it} +$

$\hat{B}_{noise}^{int}y_{kt} + \hat{C}_{noise}^{int}$ is the smoothed estimation of the measured frequency of the ik^{th} pixel that is a part of the $N_{IPSnoise}$ value given in Eq. 16.

The number of pixels $N_{IPSnoise}$ determining the set \tilde{U}_{noise} is reduced on its quantity, for which the condition (Eq. 18) is not satisfying. The process is repeated until one of the following conditions is completed: 1) the module of difference of the two related values of standard deviations becomes less than a certain value; 2) the number of pixels $N_{IPSnoise}$ becomes less than a given number; 3) the number of iterations exceeds a predetermined limit.

The next step is as follows: the obtained values of the integral parameters of the flat interference component are subtracted from the object signal of the given AIFP:

$$\nu_{ikts}^* = \nu_{ikts}^* - (\hat{A}_{noise}^{int}x_{its} + \hat{B}_{noise}^{int}y_{kts} + \hat{C}_{noise}^{int}), \quad (19)$$

where ν_{ikts}^* is the measured frequency of the photons hitting the ik^{th} pixel from the AIFP area; x_{its} and y_{kts} are the angular coordinates of the ik^{th} pixel from the AIFP area.

The AIFP area for the calculation of the flat interference component of the object image is set by the operator (the default 31×31 pixels). If the size of the object image is larger for this area, then the size of the area for the flat interference component is taken as the size of the object image multiplied by two (it is also set by the operator). As for the area of frame for fitting, we note that the fitting is carried out on the pixels that belong to the object image. Determination of these pixels is conducted through the delineation procedure, i.e. the fitting is carried out not for the fixed area but for the area which depends on the size of the object image.

The principal stages of the object image processing in the CoLiTec software are demonstrated at the pipeline in Fig. 1. They include: a) exclusion of stationary objects; b) detection of moving objects; c) analysis of moving objects, where A1, A2 and A3 outline the coordinate deviations of moving objects from their trajectory. If it is necessary, the measurements can be stacked, but only un-stacked frames are statistically processed. Image service files (flat - bias - dark) can be used during the calibration process, but we offer an alignment frame option, which is commonly used. For example, to align frames, we used a high-pass Fourier filter in the earlier versions of the CoLiTec software. Currently we are using a median filtering, which has practically the same quality but it is substantially faster. To select the moving objects, the measurements (blobs) are formed in all the selected object images. After this, frames should be identified with each other and coordinates of all the measurements should be led to the basic frame.

The algorithm of the proposed method, which could be helpful to implement it, works as follows:

1. To form a studied square area of infraframe processing (AIFP) with a side of l pixels ($N_{IPS_s}=s^2$) and a square region of the presupposed existence of images of celestial objects with a side of s pixels ($s \ll l$). The centres of these regions are the local maxima of the image of the object (asteroid, comet, etc.) discovered previously.

2. To conduct a multipass MLS-estimation of parameters of the interface noise component according to Eqs. 15 and 17. Wherein, only those pixels are processed at the next MLS-estimation pass, for which the value of the relative frequency ν_{ik}^* (Eq. 1) satisfies the condition of Eq. 18. This do-while loop is repeated as long as the module of difference of the two standard deviation values obtained sequentially becomes smaller than a predetermined value.

3. To exclude the noise photons from the potentials of pixel

in a region of the presupposed existence of images of celestial objects according to Eq. 19 (MLS-estimations of parameters of the interface noise component).

4. To estimate the coordinates of the object position according to Eq. 19 on the digital image, from which the noise photons were excluded earlier. Initial values of the coordinates of object position should be equal to the coordinates of the central local maximum of the AIFP image (AIFP centre):

4.1. to calculate the coefficients of splitting λ_{ikt} according to Eq. 10;

4.2. to estimate the coordinates of object position on the CCD frame according to Eq. 9;

4.3. to get the standard deviation estimate of the photons hitting from the object according to Eq. 11;

4.4. to determine values of the weights of the discrete mix of the probability distributions according to Eq. 12;

4.5. to compare the actual value and value obtained in the previous step. If the difference between them is greater than a predetermined value, the actual value goes to the item 4.1 as estimates of the previous step; otherwise, it goes to the algorithm output as a result of its work.

The important step of the automated pipeline is also the creation of a catalogue of stationary objects (blobs) in the frame series. All the objects of this catalogue should be excluded in next stages of the processing but a few objects should be left as reference stars for astrometry. Thus, the measurements, which are absent in the catalogue of stationary objects, have been used to select the moving objects. With this aim, the original method of collecting light (collection light technology) is provided. Candidates to the small Solar system bodies (e.g. asteroids) selected by this method should have about the same brightness on different frames, and their coordinates should not deviate significantly from their average trajectory. In case of a partial occultation of a star by an asteroid, more often they stand out as two different celestial objects, wherein the position accuracies of the star and asteroid are falling. In general, the detection of an asteroid is provided at the step of blobs, while the images themselves are not involved into processing (in this course, the blobs are formed according to the object images).

4 RESULTS AND DISCUSSION

The proposed method provides accurate estimation of asteroid coordinates on a set of the CCD frames and is the basis of the CoLiTec software, which was installed at several observatories of the world since March 1, 2009 (see, also, Fig. 1).

In April, 2010, the CoLiTec was installed at the Andrushivka Astronomical Observatory (A50), Ukraine, and already in May, 2010, two asteroids were discovered (it was the first discovery of asteroids in the automatic mode at the observatories of the CIS countries). On November 27, 2010, this software was installed at the ISON-NM (H15, New Mexico, USA), and on December 10, 2010, the comet C/2010 X1 was discovered by L. Elenin. In July, 2012, the CoLiTec software was installed at the ISON-Kislovodsk (D00, Russian Federation), and on September 21, 2012, the comet C/2012 S1(ISON) was discovered by V. Nevsky and A. Novichonok, the amateurs of astronomy. The digital images of discoveries of these comets are given in Fig. 2a and Fig. 2b, respectively. As we mentioned in the Introduction, in total 4 comets and more than 1500 asteroids have been discovered with this software since 2010 (two examples of the asteroid discoveries are demonstrated in Fig. 2c and Fig. 2d, where the latter object discovered at the An-

drushivka Astronomical Observatory on April 24, 2011, is marked as unusual K11H52Y asteroid in the MPC circular).

Since this method was already being operated during the asteroid observational surveys, we are able to provide a comparative analysis of the statistic parameters of accuracy estimations by this method and other results of thirty observatories that are most productive in terms of the number of asteroid observations in 2011–2013 (Tables 1–3). The observatories, which work with only one object in the centre of the CCD frame during the calm and suitable phase of the Moon, are excluded from our analysis. The observatories, where the CoLiTec software based on this method was installed, work during gusts and when it is calm. Moreover, the method is adaptive in such a way that there is no problem in automatic processing the object images on the CCD frames in the centre and on its edges as well as to provide measurements of many objects on the single frame.

Therefore, in the years 2011–2013, such observatories as the ISON-NM Observatory (H15) (Elenin et al. (2012), Elenin et al. (2013)), Andrushivka Astronomical Observatory (A50) (Ivashchenko et al. (2011), Ivashchenko et al. (2012), Ivashchenko et al. (2013)), and ISON-Kislovodsk Observatory (D00) acted as the users of the CoLiTec software (Elenin et al. (2014)). In the ranking of the most productive observatories worldwide in 2012, based on the number of discoveries of the small Solar System bodies, the users of the CoLiTec software had the 3rd, 13th, and 22nd places, respectively. As for the final report of 2011–2012, the ISON-NM Observatory (H15) holds the 7th place both by the number of measurements and priority of discoveries.

In Table 1 to 3, the total numbers of measurements and objects (Column 3) as well as of the asteroid discoveries (Column 4) are given according to the circulars of 2011, 2012, and 2013 of the Minor Planet Center (MPC), respectively (MPC (2013)). The statistic parameters of these measurements are taken from the MPC site. The following parameters are also indicated in the tables for each observatory: diameter D of the primary mirror of the telescope, in meters (Column 5); scale S_{pix} of the pixel image, in arc seconds (Column 6); the average residuals $\bar{\Delta}_\alpha$ and $\bar{\Delta}_\delta$ of object positions in the right ascension α and declination δ at a predetermined time (Column 7); standard deviation estimations σ_α and σ_δ of object positions in the right ascension α and declination δ at a predetermined time (Column 8); standard deviation estimations σ'' of object position (Eq. 20), in arc seconds (Column 9); standard deviation estimations σ_{pix} of object position (Eq. 21), in pixels (Column 10); module of the Average Residuals of object position Measurements (Eq. 22), ARM (Column 11). To calculate some aforementioned parameters, we applied the formula as follows:

$$\sigma'' = 0,5(\sigma_\alpha + \sigma_\delta); \quad (20)$$

$$\sigma_{pix} = \frac{\sigma''}{S_{pix}}; \quad (21)$$

$$ARM = \sqrt{(\bar{\Delta}_\alpha)^2 + (\bar{\Delta}_\delta)^2}. \quad (22)$$

The data analysis related to the accuracy parameters of object position for the most productive observatories in the number of asteroids measurements in 2011–2013 is illustrated in Figure 3.

The observatory-partners of the CoLiTec program hold leading positions in their class of telescopes as related to the parameter of module of the average residuals of measurements (Figures 3a).

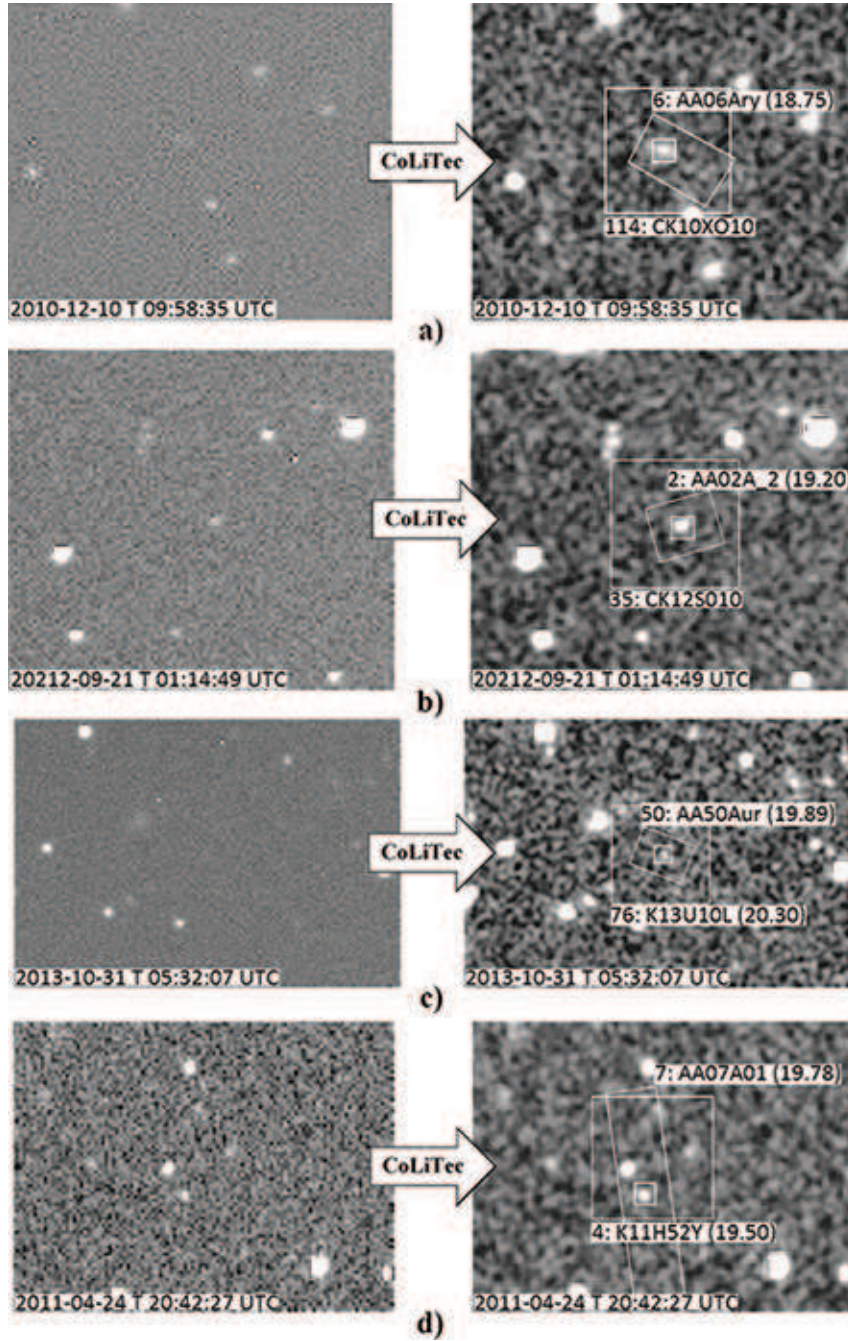


Figure 2. The most known small Solar System bodies, which were detected and discovered with the CoLiTec software based on the subpixel Gaussian model: a) the long-period Comet C/2010 X1 (Elenin), having an image size of 5 pixels, has been shifted by 7 pixels on a set of four CCD frames; b) the Comet C/2012 S1 (ISON), having an image size of 5 pixels, has been shifted by 3 pixels on a set of four CCD frames; c) Centaur object 2013 UL10, having an image size of 5-6 pixels, has been shifted by 2 pixels; d) the K11H52Y asteroid, having an image size of 5 pixels, has been shifted by 45 pixels on a set of three CCD frames (it is described as unusual in the MPC circular www.minorplanetcenter.net/mpec/K11/K11J02.html)

In 2011 and 2012, this parameter for H15 (Elenin et al. (2012)) and A50 observatories was equal to $0.06''$. At the same time, these observatories were not in the list of the best ones as related to the parameters of standard deviation estimations of object position (in arc seconds) (see, Figures 3c and 3d). In 2011, the values of standard deviation estimations σ'' of object position for the mentioned observatories were equal to $0.515''$ (H15) and $0.51''$ (A50). In 2012, these values were equal to $0.515''$ (H15), $0.49''$ (D00), and $0.48''$

(A50). The reason for such a deterioration of the results, in addition to the size of the aperture of a telescope, is the pixel scale of the used CCD matrix. To take this factor into account, the observatory-partners of the CoLiTec program decided to consider the parameter of standard deviation estimations σ_{pix} of object position, in pixels, for accurate estimation of asteroid coordinates on the CCD frame as a principal one during observations.

The parameter of standard deviation estimations σ_{pix} of the

Table 1. The accuracy parameter of thirty observatories that were the most productive in the number of asteroids measurements in 2011 according to the MPC data.

(1) N	(2) Observatory code	(3) Measurements, objects	(4) Discoveries	(5) D, m	(6) S_{pix}	(7) R.A.($\bar{\Delta}_\alpha/\sigma_\alpha$)	(8) Decl.($\bar{\Delta}_\delta/\sigma_\delta$)	(9) σ''	(10) σ_{pix}	(11) ARM
1	G96	2106367, 382737	21770	1.50	1.00	-0.01 +/- 0.32	-0.04 +/- 0.28	0.300	0.30	0.041
2	704	1956368, 279129	495	1.00	2.20	0.25 +/- 0.66	0.43 +/- 0.64	0.650	0.29	0.497
3	F51	1557902, 351923	13628	1.80	0.30	0.05 +/- 0.16	0.06 +/- 0.17	0.165	0.55	0.078
4	703	1512387, 259412	2995	0.68	2.60	-0.21 +/- 0.67	0.17 +/- 0.68	0.675	0.25	0.270
5	691	811571, 154495	8356	0.90	1.00	-0.16 +/- 0.33	0.10 +/- 0.30	0.315	0.315	0.189
6	E12	219903, 52808	327	0.50	1.80 ¹	-0.04 +/- 0.49	0.32 +/- 0.48	0.485	0.26	0.322
7	645	208656, 45961	7	2.50	0.39					
8	D29	185303, 43414	318	1.04	1.70					
9	C51	162900, 15412	23	0.40	2.75	0.06 +/- 0.57	-0.03 +/- 0.65	0.610	0.22	0.067
10	H15	154970, 37495	768	0.45	2.00	-0.03 +/- 0.49	0.06 +/- 0.54	0.515	0.25	0.067
11	106	75340, 18093	73	0.60	2.00	0.04 +/- 0.36	-0.11 +/- 0.35	0.355	0.17	0.117
12	291	70355, 19028	646	1.80	0.60	-0.13 +/- 0.36	0.15 +/- 0.27	0.315	0.52	0.191
13	J75	48469, 13209	561	0.45	1.47	-0.04 +/- 0.42	-0.14 +/- 0.40	0.410	0.28	0.146
14	644	34164, 6255	954	1.20	1.00					
15	A50	33386, 9755	72	0.60	2.06	-0.03 +/- 0.51	0.05 +/- 0.51	0.510	0.24	0.058
16	926	28578, 8460	171	0.81, 0.41	0.87	0.15 +/- 0.38	0.27 +/- 0.39	0.385	0.44	0.309
17	461	28038, 6281	782	0.60, 1.02	1.10	-0.03 +/- 0.27	0.14 +/- 0.27	0.270	0.24	0.143
18	A14	24354, 6448	115	0.50		0.08 +/- 0.41	-0.06 +/- 0.36	0.385		0.100
19	J04	23322, 6460	188	1.00	0.62 ²	0.16 +/- 0.29	0.24 +/- 0.30	0.295	0.47	0.288
20	A77	21677, 5423	318	0.50		0.027 +/- 0.63	0.22 +/- 0.50	0.565		0.348

¹Mahabal et al. (2011), ²Li et al. (1999), ³Ory et al. (2012)

(fn) Highlighted columns are CoLiTec users.

Table 2. The accuracy parameter of thirty observatories that were the most productive in the number of asteroids measurements in 2012 according to the MPC data.

(1) N	(2) Observatory code	(3) Measurements, objects	(4) Discoveries	(5) D, m	(6) S_{pix}	(7) R.A.($\bar{\Delta}_\alpha/\sigma_\alpha$)	(8) Decl.($\bar{\Delta}_\delta/\sigma_\delta$)	(9) σ''	(10) σ_{pix}	(11) ARM
1	G96	2080033, 384204	17676	1.50	1.00	0.20 +/- 0.33	0.20 +/- 0.28	0.305	0.305	0.028
2	F51	1948353, 467091	13785	1.80	0.30	0.07 +/- 0.15	0.04 +/- 0.17	0.16	0.53	0.081
3	703	1723293, 282864	2278	0.68	2.60	-0.22 +/- 0.65	0.07 +/- 0.62	0.635	0.24	0.231
4	704	1681504, 262209	224	1.00	2.20	0.26 +/- 0.67	0.43 +/- 0.64	0.655	0.29	0.502
5	691	896972, 163714	7600	0.90	1.00	-0.16 +/- 0.32	0.10 +/- 0.29	0.305	0.27	0.189
6	E12	259295, 62621	430	0.50	1.80 ¹	-0.01 +/- 0.51	0.29 +/- 0.50	0.505	0.28	0.290
7	J43	102641, 22682	531	0.50 ²	1.20 ²	0.19 +/- 0.48	0.05 +/- 0.40	0.44	0.36	0.196
8	926	100161, 29986	454	0.81, 0.41	0.87	0.02 +/- 0.37	0.05 +/- 0.35	0.36	0.41	0.54
9	H15	97878, 24170	338	0.45	2.00	-0.06 +/- 0.50	-0.01 +/- 0.53	0.515	0.25	0.061
10	106	72192, 17451	120	0.60	2.00	0.04 +/- 0.36	-0.12 +/- 0.34	0.35	0.17	0.126
11	A14	57243, 16239	159	0.50		0.06 +/- 0.37	-0.02 +/- 0.32	0.345		0.063
12	J04	43209, 10708	513	1.00	0.62 ³	0.21 +/- 0.28	0.20 +/- 0.27	0.275	0.44	0.29
13	D00	31494, 7403	61	0.40	2.06	0.00 +/- 0.57	-0.06 +/- 0.41	0.49	0.23	0.06
14	291	24272, 6224	28	1.80	0.60	0.07 +/- 0.33	0.13 +/- 0.28	0.305	0.50	0.148
15	461	23847, 5615	170	0.60, 1.02	1.10	0.00 +/- 0.27	0.15 +/- 0.27	0.27	0.24	0.15
16	644	22714, 4486	332	1.20 ⁴	1.00 ⁴					
17	H21	22672, 3870	181	0.61, 0.81, 0.76	0.80 ²	0.03 +/- 0.34	0.01 +/- 0.36	0.35	0.43	0.032
18	I41	21245, 2392	1790	1.20 ⁵	1.01 ⁵	0.11 +/- 0.23	-0.03 +/- 0.23	0.23	0.22	0.114
19	A24	18940, 2412	0	0.36	1.40	0.14 +/- 0.37	0.24 +/- 0.33	0.35	0.25	0.278
22	A50	11559, 3725	13	0.60	2.07	0.25 +/- 0.50	-0.04 +/- 0.46	0.48	0.23	0.253

¹Mahabal et al. (2011), ²Ory et al. (2012), ³Abreu et al. (2011), ⁴NEAT-PALOMAR (2013), ⁵Waszczak et al. (2013)

(fn) Highlighted columns are CoLiTec users.

object position in the pixels on the CCD frame (Figures 3b; Column 10 in Tables 1-3) is used to characterise namely an efficiency of the mathematical method, which is applied for coordinate measurements. In other words, it allows the observer to be disengaged from parameters of the used CCD matrix and other devices. According to this parameter, the observatory-partners of the CoLiTec program have one of the best results among the observatories in

their class of telescopes (small aperture). In 2011 (2012), this parameter was equal to 0.25 (0.25) pixel and 0.24 (0.23) pixel for observatories H15 and A50, respectively, as well as was equal to 0.23 pixel for D00 observatory in 2012. In 2013, the accuracy of measurements of the observatories (CoLiTec partners) fell approximately 20% for all the mentioned parameters due to an error in software that was immediately fixed and corrected completely. As

Table 3. The accuracy parameter of thirty observatories that were the most productive in the number of asteroids measurements in 2013 according to the MPC data.

(1) N	(2) Observatory code	(3) Measurements, objects	(4) Discoveries	(5) D, m	(6) S_{pix}	(7) R.A.($\Delta_\alpha/\sigma_\alpha$)	(8) Decl.($\Delta_\delta/\sigma_\delta$)	(9) σ''	(10) σ_{pix}	(11) ARM
1	F51	2279609, 506894	14168	1.80	0.30	0.13 +/- 0.07	0.06 +/- 0.14	0.135	0.45	0.092
2	G96	1950642, 343808	11908	1.50	1.00	0.04 +/- 0.32	0.05 +/- 0.28	0.300	0.30	0.064
3	703	1844330, 289086	1494	0.68	2.60	-0.14 +/- 0.66	0.22 +/- 0.64	0.650	0.25	0.260
4	691	742001, 139225	5594	0.90	1.10	-0.16 +/- 0.31	0.12 +/- 0.30	0.315	0.28	0.200
5	D29	551094, 136964	262	1.04	1.70	0.03 +/- 0.53	-0.04 +/- 0.49	0.510	0.30	0.050
6	I41	440712, 52579	2270	1.20 ¹	1.01 ¹	0.06 +/- 0.18	0.02 +/- 0.17	0.175	0.17	0.063
7	E12	229747, 48026	204	0.50	1.80 ²	-0.02 +/- 0.50	0.28 +/- 0.46	0.480	0.26	0.280
8	926	179570, 53662	750	0.81, 0.41	0.87	0.15 +/- 0.39	0.10 +/- 0.36	0.375	0.43	0.180
9	J43	151983, 27006	1006	0.50 ³	1.20 ³	0.11 +/- 0.31	-0.03 +/- 0.29	0.300	0.25	0.114
10	W84	110213, 8518	4160	403, ⁴ 4	0.27 ⁴	0.13 +/- 0.13	0.14 +/- 0.13	0.130	0.48	0.191
11	H15	107989, 25282	156	0.40	2.00	0.09 +/- 0.62	0.02 +/- 0.60	0.610	0.305	0.092
12	704	81054, 17833	4	1.00	2.20	0.29 +/- 0.64	0.38 +/- 0.63	0.635	0.28	0.478
13	J04	58307, 14670	576	1.00	0.62 ⁵	0.25 +/- 0.30	0.23 +/- 0.28	0.290	0.46	0.340
14	D00	44658, 10850	34	0.40	2.06	0.01 +/- 0.72	-0.12 +/- 0.54	0.630	0.305	0.120
15	G32	36416, 4654	654	0.40	1.13	0.03 +/- 0.35	0.05 +/- 0.32	0.335	0.29	0.058
16	106	18601, 4502	67	0.60	2.00	0.04 +/- 0.39	-0.05 +/- 0.37	0.370	0.19	0.064
17	H21	16924, 2994	60	0.61, 0.81, 0.76	0.80 ⁶	0.04 +/- 0.33	-0.04 +/- 0.31	0.320	0.4	0.002
18	461	15688, 3787	110	0.60, 1.02	1.10	-0.02 +/- 0.24	0.17 +/- 0.27	0.255	0.23	0.171
19	644	15221, 3317	63	1.20 ⁷	1.00 ⁷					
20	291	15197, 4002	1	1.80	0.60	0.02 +/- 0.35	0.14 +/- 0.32	0.335	0.55	0.141

¹Waszczak et al. (2013), ²Mahabal et al. (2011), ³Ory et al. (2012), ⁴Honscheid et al. (2008), ⁵Abreu et al. (2011), ⁶Li et al. (1999), ⁷NEAT-PALOMAR (2013)
(fn) Highlighted columns are CoLiTec users.

a result, the observatory-partners of the CoLiTec program returned to their previous positions as for the indexes of measurement accuracy (see, in detail, the current MPC site). It is important to emphasise that standard deviation σ_{pix} of object position (Figures 3b) is an artificial parameter. It is not a strong objective because such factors as the exposure time, the telescope optical scheme, the height above sea level, and many others are not taken into account in it. For example, according to this parameter, the Pan-STARRS 1 observatory (F51) had lost positions, although it had the best astrometry accuracy among all the asteroid surveys. We may suggest that an implementation of our method, which is free from a possible loss of measurement information contained on the CCD frames, when using at this observatory most likely can yield the best results than that was used.

We also compared the CoLiTec software and the Astrometrica that is widely accepted among amateurs.

Both the softwares: realise such functions as frame calibration; support of astrometric and photometric catalogues of stars in the local and online modes; record the coordinate information (WCS) in the FITS-frame title; have interactive mode for the object position measurements; have a magnifier tool; have an automated search of moving objects; have a mode for visual inspection of detected moving objects; provide output of astrometric measurements in the MPC format; transfer data mode from the interface to the MPC; display the known and discovered objects on the CCD frame. However, the CoLiTec does not realise such functions as Track&Stack for adding the frame, and identification of detected moving objects with a local database MPCORB.

At the same time, unlike the Astrometrica, the CoLiTec: realises such functions as astrometric reduction of the CCD frames with large fields of view (2^{deg} or more); separates application of the reference catalogues for astrometric and photometric reductions; provides an automated search of moving faint objects (SNR 2.5); has automatic data processing; saves results on the process-

ing frames (the real detected objects; objects, which are rejected by the operator, etc.); identifies the detected moving objects with the online database MPCORB (MPC); identifies the stationary objects with database of variable stars (VSX) and galaxies (HyperLeda); has a software modular design (the ability to connect the individual modules). The CoLiTec software gives more accurate measurements of faint celestial objects as well as contain a more reliable method for identifying the frames with a reference star catalogue allowing to improve (sometimes significantly) an accuracy of the object position.

Along with the analysis of indexes of measurement accuracy (see, the current MPC site), we conducted a comparative analysis of the accuracy of both the softwares (CoLiTec vs. Astrometrica) after processing the same frame. We selected 19 series for each of the 4 frames. A preliminary analysis included 36 series. However, the rest of the series had no reliable identification with the used star catalogue. Also, we excluded frames with significant disruptions in the daily maintenance and frames taken at very high wind. All frames were obtained at the observatory ISON-NM (H15) with help of a 40-cm telescope Santel-400AN and CCD-matrix FLI ML09000-65 (3056×3056 pixels, a pixel size of 12 microns) in the period from March 4, 2014 to March 30, 2014. The exposure time was 150 seconds.

We used only such object positions, the measurements of which are included in the MPCAT-OBS archive (MPCAT-OBS). The measurements, however, were reprocessed with the CoLiTec software. To set the reference values of object positions on the time of measurements formation, we used the HORIZONS service (HORIZONS). In total, we used 2002 measurements (measurements with CoLiTec were done on 253 more). The Astrometrica in several cases issued a sign about impossibility to guarantee a reliable measurement of object position (Centroid = -1). It is often associated with an attempt to measure the position of star trails or faint objects involved with a brighter star. More than half of them

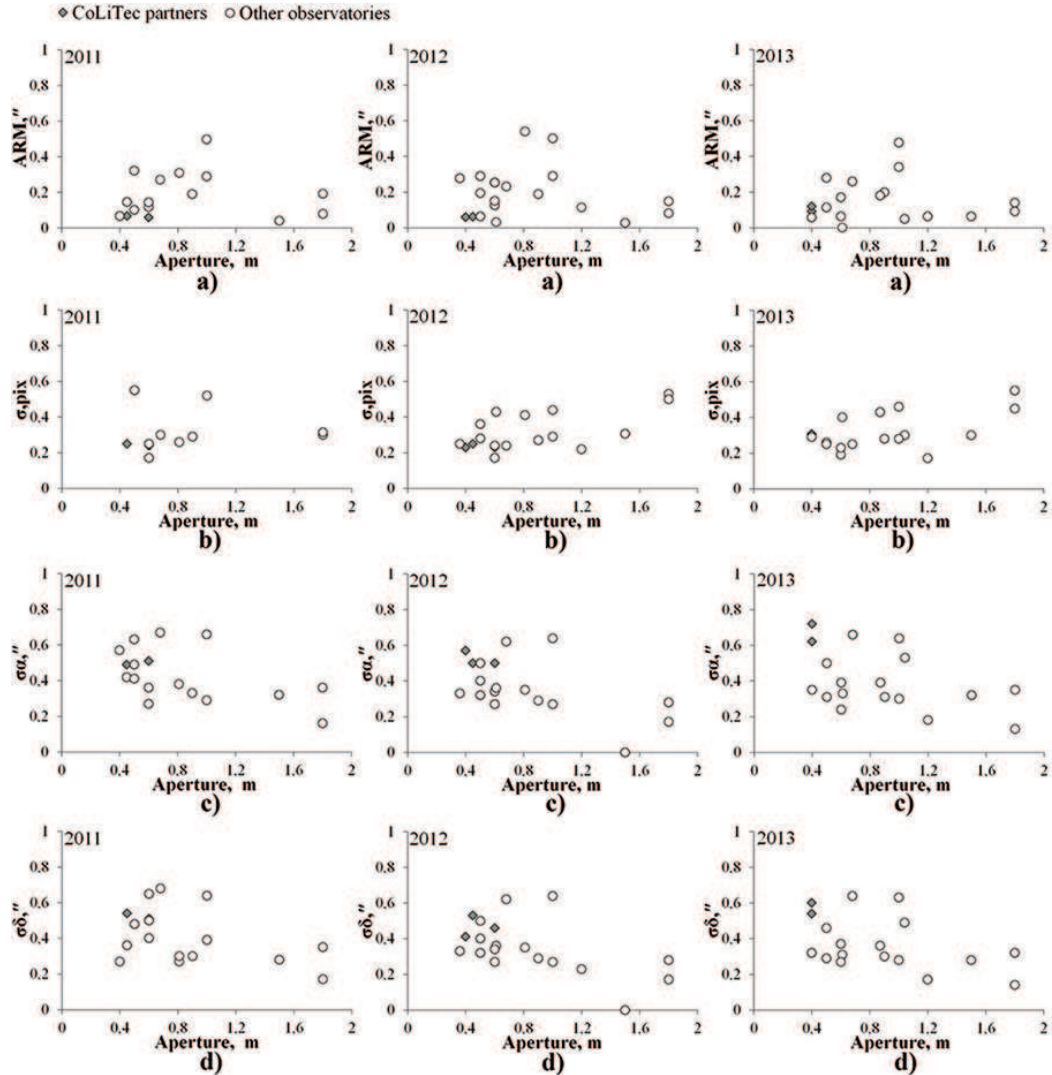


Figure 3. The comparative analysis of the accuracy parameters of object position for the most productive observatories in the number of asteroids measurements in 2011 (left), 2012 (middle), and 2013 (right) by: a) module of the average residuals of object position measurements; b) standard deviation estimations σ_{pix} of object position, in pixels; c) standard deviation estimations of object position in the right ascension, σ_α , in arcseconds; d) standard deviation estimations of object position in the declination, σ_δ , in arcseconds.

have an SNR not exceeding 3.5. The results of a comparative analysis are shown in Table 4. One can see that measurements with the Astrometrica at a low SNR have an RMS of 30–50% larger than that of the CoLiTec (see, also Fig. 4 and 5). Mean deviations in measurements with the CoLiTec and the Astrometrica are the same in general, and so these data are not shown. The more detailed comparative analysis is given in our paper (Savanevych et al. (2015)).

5 CONCLUSIONS

A new iteration method of asteroid coordinate estimation on the digital image has been developed. The method operates by continuous parameters (asteroid coordinates) in a discrete observation space (the set of pixels potential of the CCD matrix).

High rates of the CoLiTec program during 2011–2012 as concerns with the accuracy of measurements have been obtained due to the use of the subpixel Gaussian model. This model of the object image takes into account a prior form of the object image and

Table 4. Comparative analysis of the softwares CoLiTec and Astrometrica as concerns with measurements of object positions for the numbered asteroids

(1) Deviation	(2) Astrometrica	(3) CoLiTec
The average deviation of RA, ''	0,11	0,11
The average deviation of DE, ''	-0,04	-0,03
RMS deviation of RA, ''	0,77	0,50
RMS deviation of RA, ''	0,67	0,39

consequently it is adapted more easily to any forms of real image. In other words, nevertheless that a real coordinate distribution of photons hitting the pixels on the CCD frame is not known, the form of this distribution is known a priori and its parameters can be estimated according to the real object image. At that time many

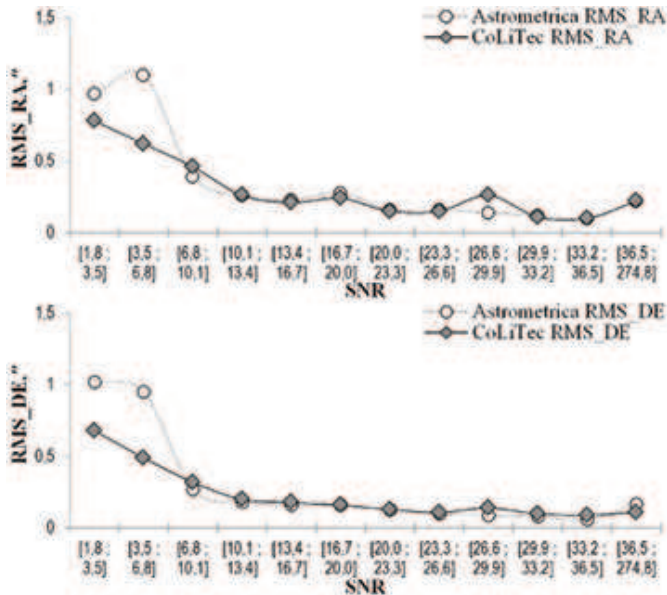


Figure 4. Distribution of deviations of the equatorial coordinates of object by SNR ranges (Astrometrica vs. CoLiTec)

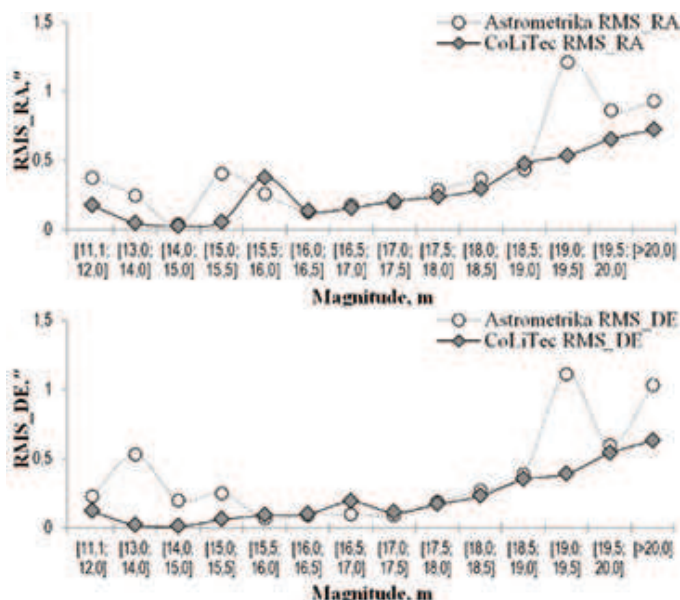


Figure 5. Distribution of deviations of the equatorial coordinates of object by magnitude ranges (Astrometrica vs. CoLiTec)

other methods mentioned in Introduction consider by default that the density of hit photons inside the pixel is uniform.

The advantages of subpixel Gaussian model become more obvious for the fainter celestial objects. Moreover, the developed method has a high measurement accuracy as well as a low calculating complexity because the maximum likelihood procedure is implemented to obtain the best fit instead of the least-squares method and Levenberg-Marquardt algorithm for the minimisation of the quadratic form.

The efficiency of the proposed method, including its advantages for accurately estimating asteroids coordinates, was con-

firmed during observations as the part of the CoLiTec (Collection Light Technology) program for automatic discoveries of asteroids and comets on a set of the CCD frames. Efficiency is a crucial factor in the discovery of near-Earth asteroids (NEA) and potentially-hazardous asteroids. Current asteroid surveys yield many images per night. It is no longer possible for the observer to quickly view these images in the blinking mode. It causes a serious difficulty for large-aperture wide-field telescopes, capturing up to several tens of asteroids in one image. The CoLiTec software solves the problem of the frame processing for asteroid surveys in a real-time mode. We compared also our software and Astrometrica, which is widely used for detecting the newly objects. Limits of measurements of CoLiTec software are wider than of Astrometrica, but that the most valuable, this expansion comes into area of extremely small SNR allowing to search the fainter Solar System small bodies (measurements with the Astrometrica at a low SNR have an RMS of 30–50% larger than that of the CoLiTec). As for the area of SNR>7, the results of CoLiTec and Astrometrica are approximately identical. However, exactly the area of extremely small SNR is more promising for the discovery of new celestial objects.

The automatically detected small Solar System bodies are subject to follow-up visual confirmation. The CoLiTec software is in use for the automated detection of asteroids at the Andrushivka Astronomical Observatory, Ukraine (since 2010), at the Russian remote observatory ISON-NM (Mayhill, New Mexico, USA) since 2010, at the observatory ISON-Kislovodsk since 2012, and at the ISON-Ussuriysk observatory since 2013 (see Tables 1–3). As the result, four comets (C/2010 X1 (Elenin) (Elenin et al. (2010)), P/2011 NO1(Elenin) (Elenin et al. (2011), Elenin et al. (2013)), C/2012 S1 (ISON) (Nevski (2012)), and P/2013 V3 (Nevski) (Nevski (2013)) as well as more than 1500 small Solar System bodies (including five NEOs, 21 Trojans of Jupiter, and one Centaur object) have been discovered.

In 2014 the CoLiTec software was recommended to all members of the Gaia-FUN-SSO network (a network for Solar System transient Objects) for analysing observations as a tool to detect faint moving objects in frames. Information about CoLiTec with link to web-site has been posted on the Gaia-FUN-SSO Wiki (<https://www.imcce.fr/gaia-fun-sso/>).

The authors thank Dr. F. Velichko for his useful comments. We are grateful to the reviewer for his helpful remarks that improved this work. We express our gratitude to Mr. W. Thuillot, coordinator of the Gaia-FUN-SSO network, for the approval of CoLiTec as a well-adapted software to the Gaia-FUN-SSO conditions of observation. We also thank Dr. Ya. Yatskiv for his support of this work in frames of the Target Program of Space Science Research of the National Academy of Science of Ukraine (2012–2016) and the Ukrainian Virtual Observatory (<http://www.ukr-vo.org>). The CoLiTec program is available through <http://colitec.neoastrosoft.com/en> (one can access to the download package http://www.neoastrosoft.com/download_en and some instructions http://www.neoastrosoft.com/documentation_en).

REFERENCES

- Abreu, D., Kuusela, J. (2013) Upgraded camera for ESA optical space surveillance system. In: 35 European Space Surveillance Conference 7–9 June 2011, INTA HQ, Madrid, Spain.
 Bauer, T. (2009). Improving the Accuracy of Position Detection of Point Light Sources on Digital Images. In: *Proceedings of*

- the IADIS Multiconference, Computer Graphics, Visualization, Computer Vision and Image Processing, Algarve, Portugal, June 20-22, 2009, p. 3-15.
- Burden, R.L., Faires, J.D. (2010) *Numerical Analysis 9th ad. Broocs/Cole*, 877.
- David, G., et al. (2013). A New Image Acquisition System for the Kitt Peak National Observatory Mosaic-1 Imager. <http://www.noao.edu/kpno/mosaic/news/SPIE7735-117r>
- Dell'Oro, A., Cellino, A. (2012). *Planetary and Space Science*, **73**, 10.
- Elenin, L., et al. (2010). *Central Bureau Electronic Telegrams*, **2384**, 1.
- Elenin, L., et al. (2011). *Central Bureau Electronic Telegrams*, **2768**, 1.
- Elenin, L., Savanevych, V., Bryukhovetskiy, A. (2012). Minor Planet Observations [H15 ISON-NM Observatory, Mayhill. *Minor Planet Circulars*, **81836**, 6.
- Elenin, L., Savanevych, V., Bryukhovetskiy, A. (2013). Comet Observations [H15 ISON-NM Observatory, Mayhill. *MPC*, **82408**, 43.
- Elenin, L., Savanevych, V., Bryukhovetskiy, A. (2013). Minor Planet Observations [H15 ISON-NM Observatory, Mayhill. *MPC*, **82692**, 1.
- Elenin, L., et al. (2014). ASPIN-ISON asteroid program: History, current state, and future prospects. In: Asteroids, Comets, Meteors 2014. Proceedings of the conference held 30 June - 4 July, 2014 in Helsinki, Finland. Edited by K. Muinonen et al..
- Faraji, H., MacLean, W.J. (2006). CCD noise removal in digital images. *Image Processing, IEEE Transactions*, **15**, 2676.
- Gary, B.L., Healy, D. (2006). Image subtraction procedure for observing faint asteroids. *Bulletin of the Minor Planets Section of the Association of Lunar and Planetary Observers*, **33**, 16.
- Gural, P.S., Larsen, J.A., Gleason, A.E. (2005). *The Astronomical Journal*, **30**, 1951.
- Harris, W.E. (1990). *Publications of the Astronomical Society of the Pacific*, **102**, 949.
- Honscheid, K., et al. (2008). The Dark Energy Camera (DECam). 34th International Conference on High Energy Physics.
- HORIZONS System. <http://ssd.jpl.nasa.gov/?horizons>
- Ivashchenko, Yu., Kyrylenko, D. (2011). Minor Planet Observations [A50 Andrushivka Astronomical Observatory]. *MPC*, **77269**, 7.
- Ivashchenko, Yu., Kyrylenko, D., Gerashchenko, O. (2012). Minor Planet Observations [A50 Andrushivka Astronomical Observatory]. *MPC*, **81732**, 6.
- Ivashchenko, Yu., Kyrylenko, D., Gerashchenko, O. (2013). Minor Planet Observations [A50 Andrushivka Astronomical Observatory]. *MPC*, **82554**, 3.
- Jogesh Babu, G., Mahabal, A.A., Djorgovski, S.G., Williams, R. (2008). Object detection in multi-epoch data. *Statistical Methodology*, **5**, 299.
- Izmailov, I.S., et al. (2010). *Astronomy Letters*, **36**, 349.
- Lafreniere, D., Marois, C. (2007). *The Astrophysical Journal*, **660**, 770.
- Li, W.D., et al (1999). The Lick Observatory Supernova Search. <http://arxiv.org/pdf/astro-ph/9912336.pdf>
- Lo, Y., Mendell, N.R., Rubin, D.B. (2001). Testing the number of components in a normal mixture. *Biometrika*, **88**, 767.
- Mahabal, A.A., et al. (2011). Discovery, classification, and scientific exploration of transient events from the Catalina Real-time Transient Survey. *Bull. Astr. Soc.*, **39**, 387.
- Miura, N., Itagaki, K., Baba, N. (2005). *The Astronomical Journal*, **130**, 1278.
- Minor Planet Center Numbered-Residuals Statistics For Observatory Codes (2013). <http://www.minorplanetcenter.net/iau/special/residuals2>
- Minor Planet Center, Rantiga Osservatorio, Tincana (2013). <http://www.minorplanetcenter.net/mpec/K13/K13H14.html>
- Minor Planet Center, Smithsonian Astrophysical Observatory (2013). <http://www.minorplanetcenter.net/mpec/K13/K13T85.html>
- Minor Planet Center, Calar Alto (2013). <http://www.minorplanetcenter.net/mpec/K13/K13Q41.html>
- MPCAT-OBS: Observation Archive: Minor Planet Checker. <http://www.minorplanetcenter.net/iau/ECS/MPCAT-OBS/MPCA>
- NASA.NEAT/PALOMAR INSTRUMENT DESCRIPTION. <http://neat.jpl.nasa.gov/neatoschincam.html>
- Nevski, V. (2012). Comet Observations [B42 Vitebsk]. *MPC*, **80063**, 14.
- Nevski, V. (2013). *Comet Observers Database*, issue 3695.
- Ory, M., et al. (2012). THE MOROCCO OUAIMEDEN SKY SURVEY, THE MOSS TELESCOPE. https://www.researchgate.net/publication/230667004_The_MOROCCO_OUAIMEDEN_SKY_SURVEY,_THE_MOSS_TELESCOPE
- Savanevych, V.E. (1999). Determination of coordinates of the statistically dependent objects on a discrete image. *Radio Electronics and Informatics*, issue 1, 4.
- Savanevych, V.E. (2006). Models and the data processing techniques for detection and estimation of parameters of the trajectories of a compact group of space small objects. Manuscript for Dr. Sci. thesis, Kharkiv: Kharkiv National University for Radio Electronics, 446 p. (in Russian).
- Savanevych, V.E., et al. (2010). Estimation of coordinates of the asteroid on the discrete image. *Radiotekhnika: All-Ukrainian Interagency scientific and engineering journal*, **162**, 78 (in Russian).
- Savanevych, V.E., et al. (2011). Program of Automatic Asteroid Search and Detection on Series of CCD-Images. In: Lunar and Planetary Inst. Technical Report, **42**, 1140.
- Savanevych, V.E., et al. (2012). *Kosmichna Nauka i Tekhnologiya*, **18**, 39.
- Savanevych, V., et al. (2014). Automated software for CCD-image processing and detection of small Solar System bodies. In: Asteroids, Comets, Meteors 2014. Proceedings of the conference held 30 June - 4 July, 2014 in Helsinki, Finland. Edited by K. Muinonen et al..
- Savanevych, V.E., et al. (2015). *Kinematics and Physics of Celestial Bodies*, **31**, 64.
- O'Sullivan, C.M.M., et al. (2000). The Mesospheric Sodium Layer at Calar Alto, Spain. <http://citeseerx.ist.psu.edu/viewdoc/download?doi=10.1.1.103.103>
- Vavilova, I.B., et al. (2011). *Kosmichna Nauka i Tekhnologiya*, **17**, 74.
- Vavilova, I.B., et al. (2012). *Kinematics and Physics of Celestial Bodies*, **28**, 85.
- Vavilova, I.B., et al. (2012). *Baltic Astronomy*, **21**, 356.
- Veres, P., Jedicke, R. (2012). *Publications of the Astronomical Society of the Pacific*, **124**, 1197.
- Waszczak, A., et al. (2013). *Mon. Not. R. Astron. Soc.*, **433**, 3115.
- Zacharias, N. (2010). *The Astronomical Journal*, **139**, 2208.
- Yanagisawa, T. et al. (2005). *Publications of the Astronomical Society of Japan*, **57**, 399.